

Direct Measurement of Aluminum Uptake and Distribution in Single Cells of *Chara corallina*¹

Gregory J. Taylor*, Julie L. McDonald-Stephens, Douglas B. Hunter, Paul M. Bertsch, David Elmore, Zdenko Rengel, and Robert J. Reid

Department of Biological Sciences, University of Alberta, Edmonton, Alberta, Canada T6G 2E9 (G.J.T., J.L.M.-S.); Advanced Analytical Center for Environmental Studies, Savannah River Ecology Laboratory, The University of Georgia, Aiken, South Carolina 29801 (D.B.H., P.M.B.); Purdue Rare Isotope Measurement Laboratory, Purdue University, West Lafayette, Indiana 47907-1396 (D.E.); Soil Science and Plant Nutrition, Faculty of Agriculture, University of Western Australia, Perth, Western Australia 6907, Australia (Z.R.); and Department of Botany, University of Adelaide, Adelaide, South Australia 5005, Australia (R.J.R.)

Quantitative information on the uptake and distribution of Al at the cellular level is required to understand mechanisms of Al toxicity, but direct measurement of uptake across the plasma membrane has remained elusive. We measured rates of Al transport across membranes in single cells of *Chara corallina* using the rare ²⁶Al isotope, an emerging technology (accelerator mass spectrometry), and a surgical technique for isolating subcellular compartments. Accumulation of Al in the cell wall dominated total uptake (71–318 $\mu\text{g m}^{-2} \text{min}^{-1}$), although transport across the plasma membrane was detectable (71–540 $\text{ng m}^{-2} \text{min}^{-1}$) within 30 min of exposure. Transport across the tonoplast was initially negligible, but accelerated to rates approximating uptake across the plasma membrane. The avacuolate protoplasm showed signs of saturation after 60 min, but continued movement across the plasma membrane was supported by sequestration in the vacuole. Saturation of all compartments was observed after 12 to 24 h. Accumulation of Al in the cell wall reflected variation in $\{\text{Al}^{3+}\}$ induced by changes in Al supply or complexing ligands, but was unaffected by pH. In contrast, transport across the plasma membrane peaked at pH 4.3 and increased when $\{\text{Al}^{3+}\}$ was reduced by complexing ligands. Cold temperature (4°C) reduced accumulation in the cell wall and protoplasm, whereas 2,4-dinitrophenol and *m*-chlorocarbonylcyanidephenyl hydrazone increased membrane transport by 12- to 13-fold. Our data suggest that the cell wall is the major site of Al accumulation. Nonetheless, membrane transport occurs within minutes of exposure and is supported by subsequent sequestration in the vacuole. The rapid delivery of Al to the protoplasm suggests that intracellular lesions may be possible.

Al toxicity is a major factor limiting growth of plants on a worldwide basis. Despite a vast research effort focusing on this problem, the primary toxic lesions and mechanisms involved in resistance to Al remain largely unknown (Taylor, 1988, 1991). Al exerts a toxic effect within minutes of exposure, but controversy remains as to whether these effects reflect cytosolic or extracytosolic injuries (Kochian, 1995; Rengel, 1996). Similarly, a number of resistance mechanisms have been proposed, but it is not clear to what extent detoxification of Al at cytosolic or extracytosolic sites contributes to resistance to Al in plants (Taylor, 1991; Kochian, 1995). To address these important questions and develop a broader understanding of the nature of Al transport across biological membranes, quantitative information about the uptake and distribution of Al at the cellular level is

required. At present, we do not know which molecular forms of Al are capable of crossing membranes, what rates of transport might be realized, or the time course over which transport occurs. The mechanistic basis of Al transport and the overall subcellular distribution remain speculative.

Our understanding of Al transport across biological membranes has been hindered by several factors, including the complex aqueous coordination chemistry of Al, its propensity to bind tightly to cell walls, the lack of an affordable and suitable isotope, and the lack of sensitive analytical techniques for detecting the low levels of Al associated with subcellular compartments. These barriers have affected research in a number of different ways. For example, microanalytical studies employing electron probe x-ray microanalysis have suggested that Al accumulates primarily in the cell wall (Hodson and Wilkins, 1991; Delhaize et al., 1993a; Marienfeld et al., 1995). Unfortunately, the limited sensitivity of this technique dictates use of long exposure times (>24 h) at concentrations of Al that may be conducive to precipitation or polymerization of Al in the apoplasm. Limited spatial resolution and sensitivity may also preclude detection of the low levels of Al associated with intracellular compartments. Although a recent study

¹ This research was supported by the Natural Sciences and Engineering Research Council of Canada Collaborative Project Grants Program, by the U.S. Department of Energy (grant no. DE-FC09-96SR18546 to the University of Georgia Research Foundation), by Southern California Edison, and by the University of Alberta Central Research Fund.

* Corresponding author; e-mail gregory.taylor@ualberta.ca; fax 780-492-9234.

claimed detection of intracellular Al in roots of wheat (*Triticum aestivum*) using electron probe x-ray microanalysis (Delhaize et al., 1993a), these results have been questioned on the basis of insufficient spatial resolution (Lazof et al., 1994).

Short-term kinetic studies have also been used as a tool to investigate Al uptake, with Al being detected by fluorescence spectroscopy (Tice et al., 1992; Vitorello and Haug, 1996, 1997) or graphite furnace atomic absorption spectrophotometry (GFAAS; Zhang and Taylor, 1989, 1990, 1991; Rincon and Gonzales, 1992; Delhaize et al., 1993a; Archambault et al., 1996a, 1996b; Samuels et al., 1997). Questions have been raised about the use of fluorophores, which may not be able to detect Al tightly bound to biological ligands. This could lead to an underestimation of Al associated with cell wall material (Archambault et al., 1996a). Perhaps more importantly, these time-dependent studies all depend on the assignment of kinetic fractions to specific cellular pools. Al uptake is typically biphasic, with a rapid, non-linear phase of uptake superimposed over a phase where uptake is linear with time (Zhang and Taylor, 1989). Although traditional interpretation of kinetic data suggests that the linear phase represents uptake across the plasma membrane, recent studies demonstrate that this phase of uptake may also include nonexchangeable Al in the cell wall (Zhang and Taylor, 1990; Tice et al., 1992; Archambault et al., 1996a). Modification of experimental conditions can minimize the contribution of cell wall binding to linear phase accumulation (Archambault et al., 1996a, 1996b), but unambiguous assignment of kinetic fractions remains elusive.

One of the most convincing arguments for the presence of intracellular Al has been provided using secondary ion mass spectrometry to localize sites of Al accumulation in roots after short-term (30-min) exposure (Lazof et al., 1994). This technique unfortunately can only provide semiquantitative estimates of Al accumulation that are based on a number of assumptions that remain to be tested (Lazof et al., 1996).

As a group, these studies suggest that Al is capable of crossing a biological membrane, but significant barriers have prevented direct, unambiguous measurements of transport rates. We have overcome these barriers by using a more direct approach involving the use of the rare ^{26}Al isotope, an emerging technology (accelerator mass spectrometry [AMS]), and a unique experimental system (giant internodal cells of *C. corallina*) in which subcellular fractions can be surgically isolated with minimal risk of cross-contamination. Our approach has provided the first direct measurement of Al transport across a plasma membrane and tonoplast in single cells. We also used this system to determine the effects of pH, Al speciation, and metabolic inhibitors on accumulation of Al in subcellular compartments.

RESULTS AND DISCUSSION

Short-Term Kinetic Experiments

Our first experiments made use of ^{27}Al -GFAAS to measure Al in the cell wall (total, nonexchangeable) and protoplasm (including the vacuole) from single cells of *C. corallina*. Accumulation of Al in the cell wall dominated uptake, with rates of total accumulation reaching $187 \mu\text{g m}^{-2} \text{min}^{-1}$ during the first 30 min, before leveling off to a constant rate of $117 \mu\text{g m}^{-2} \text{min}^{-1}$ (Fig. 1). When uptake was followed by a 30-min desorption in citric acid, rates of accumulation were $120 \mu\text{g m}^{-2} \text{min}^{-1}$ during the first 30 min followed by a constant rate of $87 \mu\text{g m}^{-2} \text{min}^{-1}$ (Fig. 1). Neither total nor nonexchangeable Al in the cell wall showed any sign of saturation during the 3-h exposure period, suggesting that the interaction of Al with cell wall material in living cells either occurs very slowly or is more than a simple, passive exchange process. In contrast to previous results with wheat (Archambault et al., 1996a), citric acid removed only 30% of total Al accumulated over 180 min. This could reflect differences in the chemical environment of the apoplasm between these two species, or differences in techniques used for isolation of the cell wall (surgery versus fractionation). Preliminary experiments in our lab suggest that the former possibility is the most likely. When cell walls of *C. corallina* were isolated using the surgical technique described here and the cell fractionation techniques described by Archambault et al. (1996a), the majority of Al associated with the cell wall was found to be nonexchangeable in both cases (data not shown). The suggestion that the cell wall environment of these two organisms might be different is plausible. These

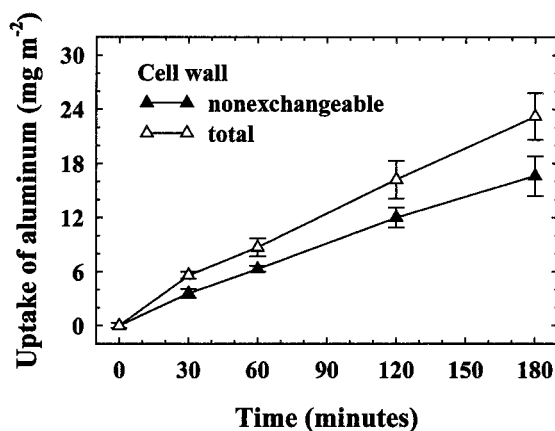


Figure 1. Short-term (180-min) time course of Al accumulation in the cell wall (total and nonexchangeable) of single cells of *C. corallina* as measured by ^{27}Al -GFAAS. Single cells were mounted in each of 15, three-compartment chambers, with the center compartment containing 110 mL of $50 \mu\text{M AlCl}_3$ in 0.4 mM CaCl_2 (pH 4.3). Following the uptake period, isolated cell walls were desorbed for 30 min in 1.0 mM citric acid (pH 4.3; 4°C) to estimate nonexchangeable Al. Values represent the means \pm SE of three replicates. Al in protoplasmic fractions was not detectable using ^{27}Al -GFAAS.

are two distantly related species with different growth forms and habitats, each of which could have an influence on the structure and composition of the cell wall. Since our goal was to determine if Al was capable of crossing biological membranes, the factors accounting for the observed differences in accumulation of total and nonexchangeable Al in the cell wall of wheat and *C. corallina* were not explored.

Accumulation of Al in the protoplasm was not detectable using ^{27}Al -GFAAS. This demonstrates the limitations of using ^{27}Al -GFAAS for analysis of short-term Al accumulation in subcellular fractions from single cells, a conclusion consistent with previous work making use of more conventional methods for detection of Al (for example GFAAS and fluorometric analyses; Reid et al., 1996).

The inadequate sensitivity of conventional techniques for detection of Al dictated the use of a novel approach. We explored the possibility of using isotopic decay for detection. Methods are currently available for generating ^{28}Al and ^{29}Al by proton irradiation of Si (Alexandrov et al., 1988), but the half-lives for these isotopes are 6.5 and 2.25 min, respectively. With the exception of ^{26}Al , all other radioactive Al isotopes have half-lives in the range of seconds. Thus, ^{26}Al is the only Al isotope well suited for tracer work (Flarend and Elmore, 1997). This unique isotope was first produced at the U.S. Department of Energy's Los Alamos National Laboratory by bombarding ^{27}Al with high-energy protons. It is a β - and γ -emitter, but the long half-life (approximately 7.3×10^5 years), modest world supply, and high cost make conventional γ counting impractical. Furthermore, conventional mass spectrometry does not provide sufficient sensitivity to distinguish ^{26}Al from other molecules and atoms with similar mass-to-charge ratios (Flarend and Elmore, 1997). Fortunately, AMS provides a technology for measuring rare, long-lived isotopes. AMS differs from conventional mass spectrometry in that charged atomic and molecular ions are accelerated to mega-electron volt energies as opposed to kilo-electron volt. This provides sufficient sensitivity to remove molecular and isobaric interference and resolve ^{26}Al from ^{27}Al at atom ratios as low as 10^{-14} . Using standard operating procedures, ^{26}Al can be detected in the attogram (10^{-17} g) range (Elmore and Phillips, 1987; Flarend and Elmore, 1997). This provides sufficient sensitivity to detect Al in subcellular fractions isolated from single cells that have been exposed to realistic environmental conditions for short periods of time. Unfortunately, the high costs associated with this technique have limited its application. Although ^{26}Al -AMS is beginning to play a role in several research fields (Flarend and Elmore 1997; Flarend et al., 1999; Yokel et al., 1999), to our knowledge this is the first reported use of ^{26}Al -AMS in a plant system.

In our experiments with ^{26}Al , uptake was once again dominated by accumulation in the cell wall,

which showed no signs of saturation during a 180-min exposure period (Fig. 2A). In contrast to our experiments using GFAAS, we were able to clearly detect Al in the protoplasmic fraction (Fig. 2B). Quantitative measures of Al accumulation in the cell wall and protoplasm showed some variation between experiments. In a series of four independent experiments (including the one presented in Fig. 2), rates of Al accumulation in the protoplasm varied between 71 and $540 \text{ ng m}^{-2} \text{ min}^{-1}$ and rates of Al accumulation in the cell wall varied between 71 and $318 \text{ } \mu\text{g m}^{-2} \text{ min}^{-1}$. Quantitative differences between

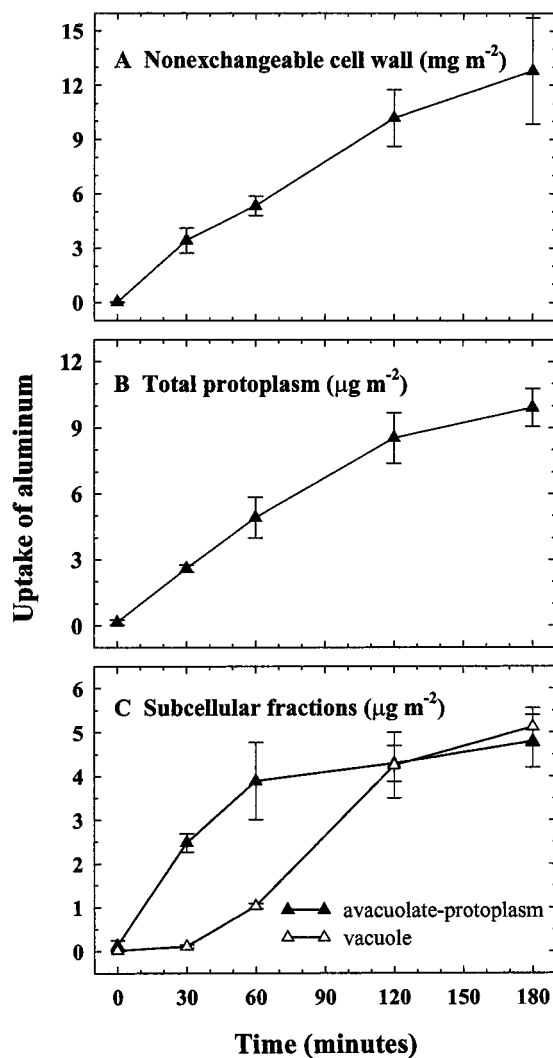


Figure 2. Short-term (180-min) time course of Al accumulation within subcellular fractions (nonexchangeable cell wall [A], total protoplasm [B], and avacolate-protoplasm and vacuoles [C]) of single cells of *C. corallina* as measured by ^{26}Al -AMS. Single cells were mounted in each of 15, three-compartment chambers, with the center compartment containing 110 mL of $50 \text{ } \mu\text{M}$ AlCl_3 in 0.4 mM CaCl_2 spiked with 75 pCi of ^{26}Al (pH 4.3). Following the uptake period, isolated cell walls were desorbed for 30 min in 1.0 mM citric acid to estimate nonexchangeable Al (pH 4.3; 4°C). Values represent the means \pm SE of three replicates. Note difference in axes scales in A (mg m^{-2}) compared to B and C ($\text{ } \mu\text{g m}^{-2}$).

experiments could reflect differences in cell maturity at the time of experiments, time after excision of internodes, the age of stock cultures, and the environmental conditions of culture growth, all of which are known to affect transport of calcium in this experimental system (Reid and Smith, 1992b). Despite this variation, accumulation of Al in the protoplasm always accounted for less than 0.5% of total uptake. This value is lower than values previously reported in the literature, perhaps reflecting different species, experimental conditions, or detection techniques (with varying potentials for cross-contamination) used in these studies.

In the absence of direct quantitative information about the movement of Al at the cellular level, several authors have speculated that Al may not appear in the protoplasm immediately upon exposure (Rengel, 1992, 1996; Marienfeld et al., 1995). The cell wall is a large sink for Al and this could play a role in restricting access of polyvalent ions to the membrane surface. In addition, it has been suggested that cationic Al species may not move readily across the plasma membrane. Thus, several authors have emphasized the importance of extracellular injury in plant response to Al (Horst, 1995; Reid et al., 1996). Our data suggest that this interpretation could be premature. We see no evidence of a lag time before Al appears in the protoplasm. Accumulation is detected within 30 min and is linear through time zero (Fig. 2B). Although our data do not exclude the possibility of extracellular lesions being a primary factor in the response to Al stress, the rapid appearance of Al within the protoplasm suggests that intracellular lesions could also play a role in toxicity.

In addition to providing the first direct, quantitative measure of Al transport across a plasma membrane, the ^{26}Al -AMS technique has provided us with the only quantitative measure of Al transport across the tonoplast. These data (Fig. 2C) are in striking contrast to the rapid appearance of Al in the total protoplasm (Fig. 2B) or avacuolate protoplasm (Fig. 2C). Movement of Al across the tonoplast to the vacuole is limited during the first 30 min of exposure, before accelerating to a rate ($46 \text{ ng m}^{-2} \text{ min}^{-1}$) that approximates the rate of movement across the plasma membrane ($71 \text{ ng m}^{-2} \text{ min}^{-1}$; Fig. 2C). This suggests that Al may have to accumulate in the cytoplasm before uptake across the tonoplast can occur. Alternatively, induction of a transport system capable of moving Al across the tonoplast may be required. Given predictions about the limited solubility of Al in the cytoplasm and its propensity to bind to biological ligands (Taylor, 1988, 1991), the nature of such a transport system, if it indeed exists, can only be speculative.

When data are expressed as accumulation of Al in the total protoplasm, little evidence (Fig. 2B) of transport saturation is evident over the 3-h experimental period. However, when accumulation in the avacu-

olate protoplasm and vacuole are measured independently (Fig. 2C), evidence of saturation becomes apparent. Accumulation of Al in the avacuolate protoplasm proceeds at a rate of $63 \text{ ng m}^{-2} \text{ min}^{-1}$ for 60 min before declining to $8 \text{ ng m}^{-2} \text{ min}^{-1}$ for the remainder of the experimental period (Fig. 2C). The declining rate of Al accumulation in the avacuolate protoplasm initially reflects sequestration of Al in the vacuole, since transport of Al across the plasma membrane into the total protoplasm (Fig. 2B) is constant over the first 2 h of exposure. During this period, sequestration of Al in the vacuole serves to support uptake across the plasma membrane. Subsequently, the rate of Al accumulation in the vacuole begins to decline (Fig. 2C). At this point, rates of accumulation in the vacuole ($14 \text{ ng m}^{-2} \text{ min}^{-1}$) and avacuolate protoplasm ($9 \text{ ng m}^{-2} \text{ min}^{-1}$) are similar and net transport across the plasma membrane declines (Fig. 2B).

Long-Term Kinetic Experiments

To evaluate the possibility of saturation in this single-cell system, we monitored accumulation in the cell wall, total protoplasm, avacuolate protoplasm, and vacuole over 72 h. These long-term data show greater variability than our short-term data, perhaps reflecting changes in the functional integrity of individual cells during long-term exposure to stressful environmental conditions. Nonetheless, a common trend was apparent in all fractions. Accumulation was rapid at the onset of exposure (<1 h), before declining to negligible levels. No net accumulation was observed in any fraction after 24 h of exposure (Fig. 3). Saturation of uptake is not surprising, since single cells are finite sinks for Al accumulation. However, we are intrigued by the length of time (approximately 12 h) required for saturation of the cell wall, which has typically been thought to occur within the first 30 min of exposure (McDonald-Stephens and Taylor, 1995). The interaction between Al and the cell wall must include more than a rapid, passive exchange with ions bound to cell wall cation exchange sites.

The Effects of pH and Al Speciation

Al phytotoxicity is influenced by the pH of exposure solutions (Blamey et al., 1993; Godbold et al., 1995), perhaps reflecting pH-dependent changes in Al speciation (Kinraide, 1991). We measured the accumulation of Al in the cell wall and protoplasm over a pH range from 3.7 to 5.2. Transport across the plasma membrane showed a clear maximum at pH 4.3 ($176 \text{ ng m}^{-2} \text{ min}^{-1}$; Fig. 4B). Rates of transport were approximately 1 order of magnitude lower at pH 3.7 and 5.2. As pH decreased from 5.2 to 4.3, rates of transport reflected predicted $\{\text{Al}^{3+}\}$ in solution, which increased from a low of $0.2 \mu\text{M}$ at pH 5.2, to

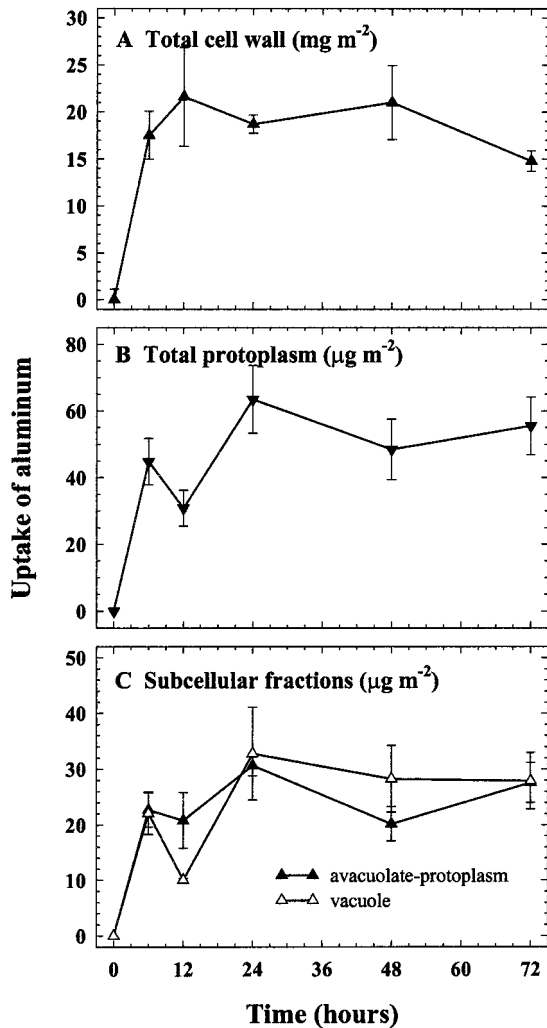


Figure 3. Long-term (72-h) time course of Al accumulation within subcellular fractions (total cell wall [A], total protoplasm [B], and avacuolate-protoplasm and vacuoles [C]) of single cells of *C. corallina* as measured by ²⁶Al-AMS. Single cells were mounted in each of 18, three-compartment chambers, with the center compartment containing 110 mL of 50 μM AlCl₃ in 0.4 mM CaCl₂ spiked with 75 pCi of ²⁶Al (pH 4.3). Values represent the means ± SE of three replicates. Note difference in axes scales in A (mg m⁻²) compared to B and C (μg m⁻²).

28.6 μM at pH 4.3 (Fig. 4D). As pH declined further to 3.7, the rate of transport fell to 23 ng m⁻² min⁻¹, despite a relatively constant predicted {Al³⁺} (28.6–32.1 μM; Fig. 4A). The strong transport maximum at pH 4.3 suggests that Al³⁺ may be the most membrane-mobile species in the absence of ligands other than OH. The decline in Al transport at low pH could reflect competition between Al³⁺ and H⁺ for binding sites at the cell surface (Kinraide et al., 1992). This idea is supported by several studies that reported amelioration of Al³⁺ toxicity by H⁺ (Kinraide, 1991; Kinraide et al., 1992). The relationship between uptake across the plasma membrane and soluble monomeric Al (pyrocatechol violet method- [PCV] reactive Al) was less clear. Activities of measured mono-

meric Al species did not begin to decline until the pH was greater than 4.6 (Fig. 4C).

A number of authors have suggested that proton amelioration of Al toxicity reflects reduced accumulation of Al in the apoplast (Klotz and Horst, 1988; Godbold et al., 1995). However, whereas transport of Al across the plasma membrane was sensitive to changes in solution pH, accumulation of Al in the cell wall was relatively unaffected (Fig. 4A). The rate of

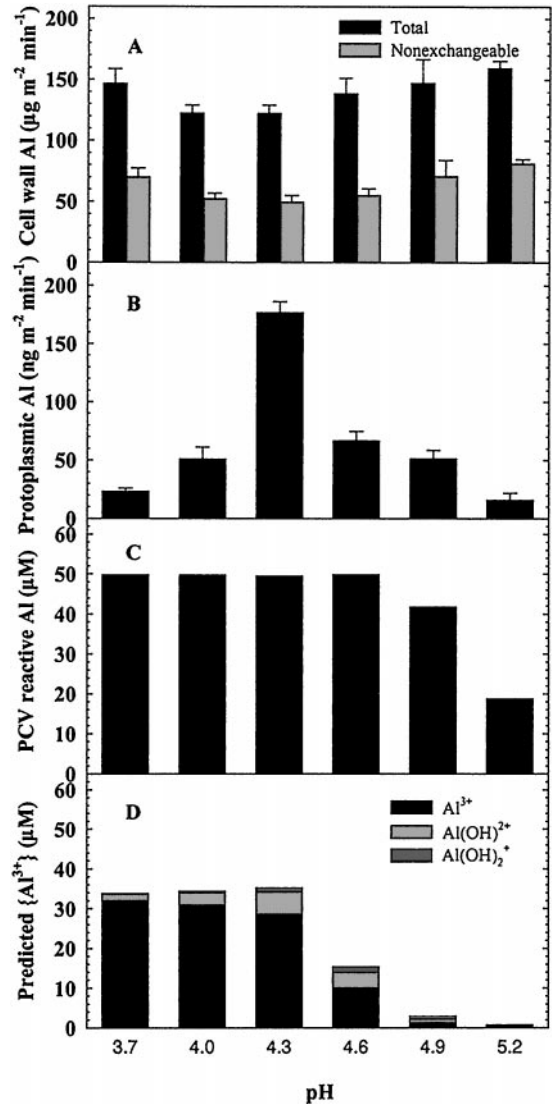


Figure 4. Accumulation of Al within subcellular fractions (total and nonexchangeable cell wall [A] and total protoplasm [B]) of single cells of *C. corallina* as measured by GFAAS and ²⁶Al-AMS in response to changes in pH of exposure solutions. Single cells were mounted in each of 18, three-compartment chambers, with the center compartment containing 110 mL of 50 μM AlCl₃ in 0.4 mM CaCl₂ spiked with 50 pCi of ²⁶Al (pH 3.7–5.2). Total soluble Al in solution (C) was measured using the PCV method. Predicted activities of monomeric species of Al in solution (D) were independently calculated using GEOCHEM-PC, version 2.0. Values represent the means ± SE of three replicates. Note difference in axes scales between A (μg m⁻² min⁻¹) and B (ng m⁻² min⁻¹).

uptake ranged from 122 to 159 $\text{ng m}^{-2} \text{min}^{-1}$ for total Al and from 50 to 81 $\text{ng m}^{-2} \text{min}^{-1}$ for nonexchangeable Al. The lack of a pH effect may suggest that accumulation of Al in the cell wall is not influenced by either $\{\text{Al}^{3+}\}$ (Fig. 4D) or total soluble monomeric Al in solution (Fig. 4C) under the current conditions. Alternatively, $\{\text{Al}^{3+}\}$ may influence accumulation in the cell wall, but this effect may be masked by precipitation and/or polymerization of Al in the cell wall. A previous study with wheat suggested that conditions conducive to precipitation of Al affected the pattern of Al uptake in the cell walls of excised roots (Archambault et al., 1996a).

Considerable debate has surrounded the identity of the rhizotoxic Al species. In the absence of polynuclear Al_{13} , Al^{3+} appears to be the primary toxic species (Kinraide, 1997) and toxicity is reduced in the presence of complexing ligands such as sulfate and citrate (Ownby and Popham, 1989; Alva et al., 1991; Kinraide, 1997). Reduced toxicity in the presence of complexing agents could result from an overall reduction in charge if apoplastic lesions are involved in Al toxicity, or from reduced uptake across the membrane if intracellular lesions are involved (Rengel, 1996). Unfortunately, difficulties involved in measuring intracellular Al have hindered efforts to relate the relative toxicity of various Al species to their ability to transverse biological membranes.

The hypothesis that Al^{3+} is the most membrane-mobile species in the absence of complexing ligands (other than OH) must be viewed with caution, since our speciation data are based on the chemistry of bulk solutions, not the cell wall free space. Kinraide (1994) found that Al toxicity in wheat was more closely related to estimated ion activities at the cell membrane surface than activities in bulk solutions. We explored this issue further by examining the effect of Al supply and speciation on membrane transport. Accumulation of Al in the cell wall and protoplasm were both strongly influenced by the concentration and speciation of Al in uptake solutions (Fig. 5). Unlike our pH experiments where we did not find a relationship between $\{\text{Al}^{3+}\}$ and accumulation in the cell wall, accumulation clearly reflected predicted $\{\text{Al}^{3+}\}$ in solution, both in the presence and absence of sulfate and citrate. Any reduction in predicted $\{\text{Al}^{3+}\}$ from nominal values (Fig. 5D) resulted in a reduction in both total and nonexchangeable accumulation of Al in the cell wall (Fig. 5A). This was true when $\{\text{Al}^{3+}\}$ was reduced either by limiting the supply of total Al or by the addition of sulfate or citrate. When total Al in solution was kept constant at $50 \mu\text{M}$ but $\{\text{Al}^{3+}\}$ (nominally $28.6 \mu\text{M}$) was reduced by the addition of sulfate and citrate, accumulation of total cell wall Al decreased by 20% and 51% and accumulation of nonexchangeable cell wall Al decreased by 14% and 50%, respectively (Fig. 5A). In contrast, similar rates of accumulation were observed when cells were exposed to $50 \mu\text{M}$ AlCl_3 alone ($\{\text{Al}^{3+}\} = 28.6 \mu\text{M}$) and when total Al was increased, but $\{\text{Al}^{3+}\}$ was kept constant by addition of sulfate and citrate. The relationship between accumulation of Al in the cell wall and soluble monomeric Al (PCV-reactive Al; Fig. 5C) was less clear, presumably because AlSO_4 reacts with PCV (note comparison between $\{\text{Al}^{3+}\}$ and $\{\text{AlSO}_4\}$ predicted

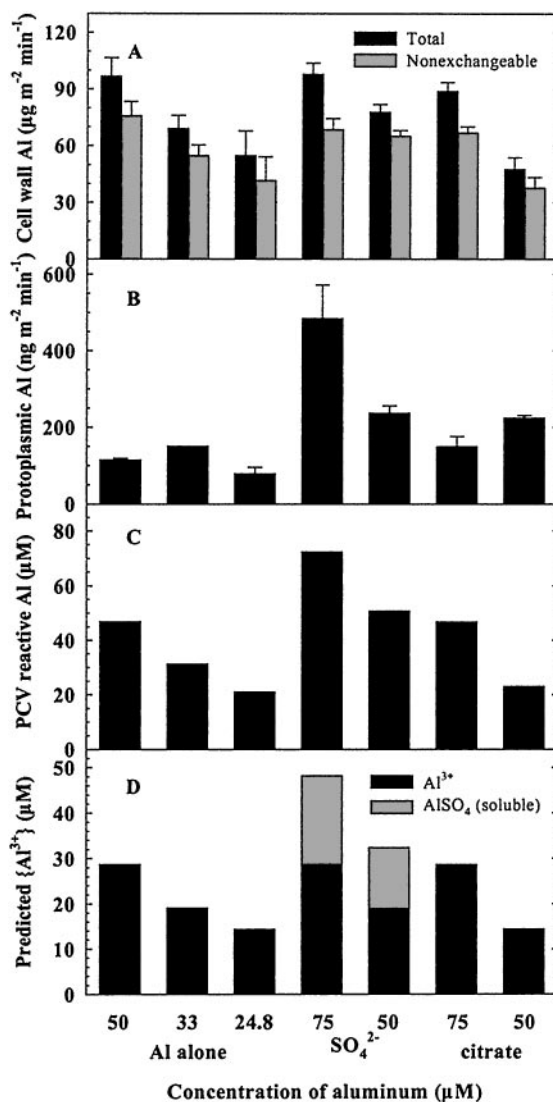


Figure 5. Accumulation of Al within subcellular fractions of single cells of *C. corallina* in response to varying supplies and sources of Al. Accumulation of Al in the cell wall (total and nonexchangeable [A] and protoplasm [B]) from solutions containing AlCl_3 alone, or AlCl_3 in the presence of sulfate and citrate (see "Materials and Methods") were measured by GFAAS and ^{26}Al -AMS. Total soluble Al in solution (C) was measured using the PCV method. Predicted activities of monomeric Al species in solution (D) were independently estimated using GEOCHEM-PC, version 2.0. Single cells were mounted in each of 21, three-compartment chambers, with the center compartment containing 110 mL of $50 \mu\text{M}$ AlCl_3 in 0.4 mM CaCl_2 spiked with 50 pCi of ^{26}Al (pH 3.7–5.2). Following the uptake period, isolated cell walls were desorbed for 30 min in 1.0 mM citric acid (pH 4.3; 4°C). Values represent the means \pm SE of three replicates. Note difference in axes scales between A ($\mu\text{g m}^{-2} \text{min}^{-1}$) and B ($\text{ng m}^{-2} \text{min}^{-1}$).

μM AlCl_3 alone ($\{\text{Al}^{3+}\} = 28.6 \mu\text{M}$) and when total Al was increased, but $\{\text{Al}^{3+}\}$ was kept constant by addition of sulfate and citrate. The relationship between accumulation of Al in the cell wall and soluble monomeric Al (PCV-reactive Al; Fig. 5C) was less clear, presumably because AlSO_4 reacts with PCV (note comparison between $\{\text{Al}^{3+}\}$ and $\{\text{AlSO}_4\}$ predicted

using GEOCHEM-PC [Parker et al., 1987; Fig. 5D] and reactive Al measured independently using the PCV method [Fig. 5C]). The effect of complexing ligands on accumulation of Al in the cell wall suggested that accumulation was strongly influenced by charge. In the presence of sulfate and citrate, Al is complexed predominantly as AlSO_4^+ and $\text{AlCit}_{\text{H}}^-$ or AlCit^0 .

In contrast to accumulation of Al in the cell wall, no clear relationship was observed between the rate of transport across the plasma membrane (Fig. 5B) and predicted $\{\text{Al}^{3+}\}$ in exposure solutions (Fig. 5D). Accumulation of Al in the protoplasm proceeded at a rate of $114 \text{ ng m}^{-2} \text{ min}^{-1}$ in the presence of $50 \mu\text{M AlCl}_3$ ($\{\text{Al}^{3+}\} = 28.6 \mu\text{M}$). Rates of accumulation increased 4.2- and 1.3-fold when total Al was increased to $75 \mu\text{M}$, but $\{\text{Al}^{3+}\}$ maintained constant in the presence of SO_4^{2-} and citrate, respectively. When total Al was kept constant, but $\{\text{Al}^{3+}\}$ was reduced in the presence of these ligands, rates of membrane transport increased by 2.1-fold in the presence of SO_4^{2-} and by 2.0-fold in the presence of citric acid. Increased rates of membrane transport observed in the presence of SO_4^{2-} and citrate suggest that complexes such as AlSO_4^+ , $\text{AlCit}_{\text{H}}^-$, or AlCit^0 may be readily transported across the plasma membrane. Several authors have suggested that AlCit^0 may provide a means by which Al may pass through biological membranes (Martin 1988; Kochian, 1995). However, this interpretation must still be viewed with caution, since our speciation analyses were based on the chemistry of bulk solutions, which may differ significantly from the cell membrane surface.

At first glance, these results appear to contradict recent evidence that suggests exudation of organic acids may be involved in resistance to Al (Miyasaka et al., 1991; Delhaize et al., 1993b; Basu et al., 1994) and the observation that complexed forms of Al are commonly found to be less toxic to root elongation in higher plants (Delhaize et al., 1993b; Kinraide, 1997; Ma and Miyasaka, 1998). It is important to recognize, however, that a link between membrane transport of Al and expression of toxicity remains to be estab-

lished. If extracellular lesions do indeed play an important role in expression of toxicity, exudation of organic ligands could protect plants from extracellular Al injury even with increasing uptake across the plasma membrane.

The Effects of Inhibitors

Flux rates across the plasma membrane and into the cell wall were also measured in the presence or absence of a variety of inhibitors. When cells were exposed to Al at 4°C , total accumulation into the cell wall, nonexchangeable accumulation in the cell wall, and uptake across the plasma membrane were reduced by 40.8%, 38.6%, and 57.1%, respectively, compared to results at 22°C (Table I). Similar results were also found when roots of wheat were exposed to AlCl_3 at low temperature (Zhang and Taylor, 1990). In contrast to these effects, accumulation in the protoplasm was 13- and 14-fold higher in the presence of $100 \mu\text{M}$ 2,4-dinitrophenol (DNP) and $10 \mu\text{M}$ *m*-chlorocarbonylcyanidephenol hydrazone (CCCP), respectively, than in the presence of Al alone. Accumulation of total and nonexchangeable Al in the cell wall was relatively unaffected (Table I), which suggests that uptake into this compartment is not energy dependent.

These results are consistent with several studies using cell wall material isolated from roots of wheat, which reported no effect of DNP in Al-sensitive cultivars (Zhang and Taylor, 1989, 1991). Several studies have reported increased accumulation of Al in roots in the presence of metabolic inhibitors (Rahat and Reinhold, 1983; Wagatsuma, 1983; Zhang and Taylor 1989, 1991), but the location of this absorbed Al remains speculative. It is difficult to draw conclusions about how such inhibitors may affect Al uptake. These inhibitors induce a variety of effects, including inhibition of oxidative phosphorylation, reduction of cellular ATP levels, destruction of the proton gradient across the membrane, and disruption of membrane structure and permeability (Zhang and Taylor, 1989). However, the fact that DNP and CCCP both

Table 1. Accumulation of Al in subcellular fractions (total and nonexchangeable cell wall, total protoplasm) of single cells of *C. corallina* as measured by ^{26}Al -AMS in the presence or absence of metabolic inhibitors

Single cells were mounted in each of 12, three-compartment chambers, with the center compartment containing 110 mL of $50 \mu\text{M AlCl}_3 \pm$ inhibitors (4°C , $100 \mu\text{M}$ DNP, or $10 \mu\text{M}$ CCCP) in 0.4 mM CaCl_2 spiked with 50 pCi of ^{26}Al (pH 4.3). Isolated cell walls were desorbed in 1.0 mM citric acid (4°C) following 180 min of uptake to estimate nonexchangeable aluminum. Values represent the means \pm se of three replicates.

Exposure Solution	Cell Fraction		
	Total cell wall	Nonexchangeable cell wall	Protoplasm
	mg m^{-2} (%)	mg m^{-2} (%)	$\mu\text{g m}^{-2}$ (%)
AlCl_3	15.7 ± 1.1 (100)	13.2 ± 1.0 (100)	7.0 ± 0.4 (100)
AlCl_3 (4°C)	9.3 ± 0.7 (59.2)	8.1 ± 0.7 (61.4)	3.0 ± 0.1 (42.9)
$\text{AlCl}_3 + \text{DNP}$	14.3 ± 0.9 (91.1)	13.2 ± 0.7 (100)	90.8 ± 10.5 (1,297)
$\text{AlCl}_3 + \text{CCCP}$	13.0 ± 1.1 (82.8)	11.6 ± 1.1 (87.9)	97.5 ± 14.2 (1,393)

stimulated uptake suggests that the proton gradient across the plasma membrane is not the only factor affecting transport. Our data do not allow us to determine whether increased uptake was a result of increased membrane permeability (Rahat and Reinhold, 1983; Wagatsuma, 1983) or disruption of a metabolism-dependent exclusion mechanism (Zhang and Taylor, 1989).

SUMMARY

To our knowledge, our data provide the first quantitative measure of Al transport across the plasma membrane and tonoplast of single cells. By making use of a unique experimental system, the rare ^{26}Al isotope, and the powerful AMS technology, we have shown that Al is capable of crossing biological membranes within minutes of exposure. This suggests that intracellular lesions could play a role in acute Al toxicity. We have also shown that the unique environment of the protoplasm does not prevent movement of Al into the vacuole, which begins after a brief lag period (30 min). Our long-term data suggest that uptake in the cell wall, avacuolate protoplasm, and vacuole saturates within 12 to 24 h of exposure. Accumulation in the cell wall and transport across the plasma membrane are also sensitive to environmental factors such as pH and complex formation.

MATERIALS AND METHODS

Kinetic Experiments

Cultures of the charophyte algae, *Chara corallina* were grown in 36-L plastic tanks on a mixture of garden soil and sand in distilled water (photon flux density = $25 \mu\text{mol m}^{-2} \text{s}^{-1}$ for a 16-h day; solution temperature = 23.5°C – 24.5°C). Single internodal cells (60–90 mm long, approximately 1 mm in diameter) were excised prior to uptake experiments and whorl cells were removed. Cells were stored overnight between filter paper moistened with a solution consisting of 1.0 mM NaCl, 0.5 mM CaCl_2 , and 0.1 mM K_2SO_4 .

Excised internodal cells were checked for vitality (as determined by the presence of cytoplasmic streaming) and vital cells were mounted in three-compartment chambers containing 0.4 mM CaCl_2 (pH 4.3) in each compartment. Following a 60-min equilibration period, solutions in central compartments were replaced with 110 mL of 50 μM AlCl_3 and 0.4 mM CaCl_2 , with or without 50 to 75 pCi of ^{26}Al (pH 4.3). Solutions in end compartments were replaced with fresh CaCl_2 without Al to minimize the potential for redistribution of Al during surgical isolation. Analysis of absorption solutions from central compartments using GFAAS confirmed that depletion never exceeded 10% of added Al. Random sampling of end compartments from each experiment showed no evidence of ^{26}Al contamination from central compartments.

Cells were removed from uptake solutions after 0 to 180 min or 0 to 72 h and subcellular compartments (cell wall and protoplasm, or cell wall, avacuolate protoplasm, and

vacuole) were surgically isolated as described by Reid and Smith (1992a). Individual cells were air-dried for 30 to 45 s to reduce turgor. The ends of cells were then excised to expose the protoplasm and a syringe was impaled into one end. A small air bubble was passed through the cell to eject the vacuole, followed by a stream of water to eject the avacuolate protoplasm. Cell walls were rinsed in 0.4 mM CaCl_2 (pH 4.3) and transferred to 20 mL of citric acid (1 mM, pH 4.3) for 30 min to remove exchangeable Al. After 30 min, cell wall sleeves were removed, rinsed with deionized water ($>18 \text{ m}\Omega$), and prepared for determination of Al by ^{27}Al -GFAAS. Isolated protoplasmic fractions from single cells were prepared for determination of Al by ^{27}Al -GFAAS or ^{26}Al -AMS. Desorption solutions were analyzed directly for Al content using GFAAS. Most experiments were replicated at least twice in some form, but due to the high costs of analyses we were unable to replicate all of our experiments in their entirety.

The Effect of pH and Al Speciation

The effect of pH on Al accumulation in subcellular fractions was examined by exposing cells to solutions containing 50 μM AlCl_3 , 0.4 mM CaCl_2 , and 50 pCi ^{26}Al (in 110 mL) for 180 min. Bulk solution pH was adjusted from pH 3.7 to 5.2 using 0.1 N HCl or 0.1 N KOH. The effects of Al supply and speciation on accumulation of Al in subcellular compartments were examined by exposing cells to three different series of solutions, each of which included 0.4 mM CaCl_2 and 50 pCi ^{26}Al (in 110 mL) at pH 4.3. In the first series, predicted $\{\text{Al}^{3+}\}$ was maintained at 28.6 μM , whereas total Al was increased in the presence of SO_4 or citric acid. This series of solutions included: (a) 50 μM AlCl_3 ; (b) 50 μM AlCl_3 , 25 μM $\text{AlK}(\text{SO}_4)_2$, and 253 μM K_2SO_4 ; and (c) 75.3 μM AlCl_3 and 25 μM citric acid. In the second series, total Al was kept constant at 50 μM and $\{\text{Al}^{3+}\}$ was reduced by the addition of SO_4 or citric acid. This series of solutions included: (a) the same 50 μM AlCl_3 treatment described above; (b) 50 μM AlCl_3 and 300 μM K_2SO_4 ; and (c) 50 μM AlCl_3 and 25 μM citric acid. In the final series, total Al was reduced to provide the levels of $\{\text{Al}^{3+}\}$ predicted for the second series. This series included: (a) the same 50 μM AlCl_3 treatment described above; (b) 33 μM AlCl_3 ; and (c) 24.8 μM AlCl_3 . Accumulation of Al in subcellular fractions was measured after 180 min of exposure.

Speciation of Al in bulk solutions was predicted using the computer program GEOCHEM-PC, version 2.0. A value of -8.8 was used in place of -8.1 for the log K value of gibbsite $[\text{Al}(\text{OH})_3]$; Kinraide and Parker, 1989) and log K values of -5.0 , -10.1 , -16.8 , and -22.7 were used for the hydrolysis of Al (Parker et al., 1987; Nordstrom and May, 1989). Empirical estimates of monomeric Al in solution were experimentally measured on independent samples using the PCV method (Menzies et al., 1992) as described by McDonald-Stephens and Taylor (1995), except that a 60-s reaction time was used due to the presence of organic ligands in solution (Kerven et al., 1989).

The Effect of Inhibitors

The effect of metabolic perturbation on Al accumulation was examined by exposing cells to solutions containing 50 μM AlCl_3 , 4 mM CaCl_2 , and 50 pCi ^{26}Al (in 110 mL; pH 4.3), with or without DNP (100 μM) or CCCP (10 μM), for 180 min. Inhibitors were dissolved in 95% (v/v) ethanol, thus aliquots of ethanol were added to all solutions (including those in end compartments) to achieve a final concentration of 0.95% (v/v). This concentration had no effect on cytoplasmic streaming or chloroplast organization, suggesting that cell vitality was not affected (Reid et al., 1996). A cold-temperature treatment was imposed by exposing cells to solutions containing 0.4 mM $\text{CaCl}_2 \pm 50 \mu\text{M}$ AlCl_3 and 50 pCi ^{26}Al at 4°C.

Determination of Al

Samples were prepared and analyzed by ^{27}Al -GFAAS using techniques described by McDonald-Stephens and Taylor (1995). For ^{26}Al -AMS analysis, protoplasmic fractions were dried, diluted with concentrated nitric acid, and mixed with a ^{27}Al carrier solution (ICP/DCP standard solution, 10,050 mg L^{-1} Al; Aldrich Chemical Company, Milwaukee, WI) to bring the ratio of ^{26}Al to ^{27}Al to approximately 5×10^{-11} . Samples were dried and ashed for 6 h at 700°C, and the resultant Al_2O_3 samples were analyzed for Al content using AMS at the Purdue Rare Isotope Measurement Laboratory (Flarend and Elmore, 1997). Appropriate blank samples were run periodically to test for possible cross-contamination between samples. Data from both ^{26}Al and ^{27}Al analyses were expressed as total Al uptake (in micro- or milligrams) per unit surface area exposed (m^{-2}) or as uptake rates (in nano- or micrograms Al) per unit surface area exposed (in square meters) per minute.

Received November 29, 1999; accepted March 17, 2000.

LITERATURE CITED

- Aleksandrov VN, Semenova MP, Semenov VG (1988) Cross sections of radionuclide production in (p, x)-reactions on aluminum and silicon. *Sov Atom Energy* **64**: 511–513
- Alva AK, Kerven GL, Edwards DG, Asher CJ (1991) Reduction in toxic aluminum to plants by sulfate complexation. *Soil Sci* **152**: 351–359
- Archambault DJ, Zhang G, Taylor GJ (1996a) A comparison of the kinetics of aluminum (Al) uptake and distribution in roots of wheat (*Triticum aestivum*) using different aluminum sources: a revision of the operational definition of symplastic aluminum. *Physiol Plant* **98**: 578–586
- Archambault DJ, Zhang G, Taylor GJ (1996b) Accumulation of aluminum in root mucilage of an aluminum-resistant and an aluminum-sensitive cultivar of wheat. *Plant Physiol* **112**: 1471–1478
- Basu U, Godbold D, Taylor GJ (1994) Aluminum resistance in *Triticum aestivum* associated with enhanced exudation of malate. *J Plant Physiol* **144**: 747–753
- Blamey FPC, Asher CJ, Kerven GL, Edwards DG (1993) Factors affecting aluminum sorption by calcium pectate. *Plant Soil* **149**: 87–94
- Delhaize E, Craig S, Beaton CD, Bennet RJ, Jagadish VC, Randall PJ (1993a) Aluminum tolerance in wheat (*Triticum aestivum* L.): I. Uptake and distribution of aluminum in root apices. *Plant Physiol* **103**: 685–693
- Delhaize E, Ryan PR, Randall PJ (1993b) Aluminum tolerance in wheat (*Triticum aestivum* L.): II. Aluminum-stimulated excretion of malic acid from root apices. *Plant Physiol* **103**: 695–702
- Elmore D, Phillips FM (1987) Accelerator mass spectrometry for measurement of long-lived radioisotopes. *Science* **236**: 543–550
- Flarend R, Elmore D (1997) Aluminum-26 as a biological tracer using accelerator mass spectrometry. In P Zatta, AC Alfrey, eds, *Aluminum in Infant's Health and Nutrition*. World Scientific, Singapore, pp 16–39
- Flarend R, Keim C, Bin T, Elmore D, Hem S, Ladisch M (1999) Analysis of aluminum-26 labeled aluminum chlorohydrate. *J Inorg Biochem* **76**: 149–152
- Godbold DL, Jentschke G, Marschner P (1995) Solution pH modifies the response of Norway spruce seedlings to aluminum. *Plant Soil* **171**: 175–178
- Hodson MJ, Wilkins DA (1991) Localization of aluminum in the roots of Norway spruce [*Picea abies* (L.) Karst.] inoculated with *Paxillus involutus* Fr. *New Phytol* **118**: 273–278
- Horst WJ (1995) The role of the apoplast in aluminum toxicity and resistance of higher plants: a review. *Z Pflanzenernahr Bodenk* **158**: 419–428
- Kerven GL, Edwards DG, Asher CJ, Hallman PS, Kokot S (1989) Aluminum determination in soil solution II: short-term colorimetric procedures for the measurement of inorganic monomeric aluminum in the presence of organic acid ligands. *Aust J Soil Res* **27**: 91–102
- Kinraide TB (1991) Identity of the rhizotoxic aluminum species. *Plant Soil* **134**: 167–178
- Kinraide TB (1994) Use of a Guoy-Chapman-Stern model for membrane-surface electrical potential to interpret some features of mineral rhizotoxicity. *Plant Physiol* **106**: 1583–1592
- Kinraide TB (1997) Reconsidering the rhizotoxicity of hydroxyl, sulphate and fluoride complexes of aluminum. *J Exp Bot* **48**: 1115–1124
- Kinraide TB, Parker DR (1989) Assessing the phytotoxicity of mononuclear hydroxy-aluminum. *Plant Cell Environ* **12**: 479–487
- Kinraide TB, Ryan PR, Kochian LV (1992) Interactive effects of Al^{3+} , H^+ , and other cations on root elongation considered in terms of cell-surface electrical potential. *Plant Physiol* **99**: 1461–1468
- Klotz F, Horst WJ (1988) Effect of ammonium and nitrate nitrogen on aluminum tolerance of soybean (*Glycine max* L.) *Plant Soil* **111**: 59–65
- Kochian LV (1995) Cellular mechanisms of aluminum toxicity and resistance in plants. *Annu Rev Plant Physiol Plant Mol Biol* **46**: 237–260

- Lazof DB, Goldsmith GJ, Ruffy TW, Linton RW** (1994) Rapid uptake of aluminum into cells of intact soybean root tips. *Plant Physiol* **106**: 1107–1114
- Lazof DB, Goldsmith GJ, Ruffy TW, Linton RW** (1996) A comparison of three developmental root regions using secondary ion mass spectrometry imaging. *Plant Physiol* **112**: 1289–1300
- Ma Z, Miyasaka SC** (1998) Oxalate exudation by taro in response to Al. *Plant Physiol* **118**: 861–865
- Marienfeld S, Lehmann H, Stelzer R** (1995) Ultrastructural investigations and EDX-analyses of Al-treated oat (*Avena sativa*) roots. *Plant Soil* **171**: 167–173
- Martin RB** (1988) Bioinorganic chemistry of aluminum. In H Sigel, ed, *Metal Ions in Biological Systems: Aluminum and Its Role in Biology*. Marcel Dekker, New York, pp 1–57
- McDonald-Stephens JL, Taylor GJ** (1995) Kinetics of aluminum uptake by cell suspensions of *Phaseolus vulgaris* L. *J Plant Physiol* **145**: 327–334
- Menzies NW, Kerven GL, Bell LC, Edwards DG** (1992) Determination of total soluble aluminum in soil solution using pyrocatechol violet, lanthanum and iron to discriminate against microparticulates and organic ligands. *Commun Soil Sci Plant Anal* **23**: 2525–2545
- Miyasaka SC, Buta JG, Howell RK, Foy CD** (1991) Mechanisms of aluminum tolerance in snapbeans. *Plant Physiol* **96**: 737–743
- Nordstrom DK, May HM** (1989) Aqueous equilibrium data for mononuclear aluminum species. In G Sposito, ed, *The Environmental Chemistry of Aluminum*. CRC Press, Boca Raton, FL, pp 29–53
- Ownby JD, Popham HR** (1989) Citrate reverses the inhibition of wheat growth caused by aluminum. *J Plant Physiol* **135**: 588–591
- Parker DR, Zelazny LW, Kinraide TB** (1987) Improvements to the program GEOCHEM. *Soil Sci Soc Am J* **51**: 488–491
- Rahat M, Reinhold L** (1983) Rb⁺ uptake by isolated pea mesophyll protoplasts in light and darkness. *Physiol Plant* **59**: 83–90
- Reid RJ, Rengel Z, Smith FA** (1996) Membrane fluxes and comparative toxicities of aluminum, scandium and gallium. *J Exp Bot* **47**: 1881–1888
- Reid RJ, Smith FA** (1992a) Measurement of calcium fluxes in plants using ⁴⁵Ca. *Planta* **186**: 558–566
- Reid RJ, Smith FA** (1992b) Regulation of calcium influx in *Chara*: effect of K⁺, pH, metabolic inhibition and calcium channel blockers. *Plant Physiol* **100**: 637–643
- Rengel Z** (1992) Role of calcium in aluminum toxicity. *New Phytol* **121**: 499–513
- Rengel Z** (1996) Uptake of aluminum by plant cells. *New Phytol* **134**: 389–406
- Rincon M, Gonzales RA** (1992) Aluminum partitioning in intact roots of aluminum-tolerant and aluminum-sensitive wheat (*Triticum aestivum* L.) cultivars. *Plant Physiol* **99**: 1021–1028
- Samuels TD, Kucukakyuz K, Rincon-Zachary M** (1997) Al partitioning patterns and root growth as related to Al sensitivity and Al tolerance in wheat. *Plant Physiol* **113**: 527–534
- Taylor GJ** (1988) The physiology of aluminum phytotoxicity. In H Sigel, ed, *Metal Ions in Biological Systems: Aluminum and Its Role in Biology*. Marcel Dekker, New York, pp 123–163
- Taylor GJ** (1991) Current views of the aluminum stress response: the physiological basis of tolerance. In DD Randall, DG Blevins, CD Miles, eds, *Current Topics in Plant Biochemistry and Physiology*. Interdisciplinary Plant Biochemistry and Physiology Program, University of Missouri, Columbia, pp 57–93
- Tice KR, Parker DR, DeMason DA** (1992) Operationally defined apoplastic and symplastic aluminum fractions in root tips of aluminum-intoxicated wheat. *Plant Physiol* **100**: 309–318
- Vitarello VA, Haug A** (1996) Short-term aluminum uptake by tobacco cells: growth dependence and evidence for internalization in a discrete peripheral region. *Physiol Plant* **97**: 536–544
- Vitarello VA, Haug A** (1997) An aluminum-morin fluorescence assay for the visualization and determination of aluminum in cultured cells of *Nicotiana tabacum* L. cv. BY-2. *Plant Sci* **122**: 35–42
- Wagatsuma T** (1983) Effect of non-metabolic conditions on uptake of aluminum by plant roots. *Soil Sci Plant Nutr* **29**: 323–333
- Yokel RA, Allen DD, Ackley DC** (1999) The distribution of aluminum into and out of the brain. *J Inorg Biochem* **76**: 127–132
- Zhang G, Taylor GJ** (1989) Kinetics of aluminum uptake by excised roots of aluminum-tolerant and aluminum-sensitive cultivars of *Triticum aestivum* L. *Plant Physiol* **91**: 1094–1099
- Zhang G, Taylor GJ** (1990) Kinetics of aluminum uptake in *Triticum aestivum* L.: identity of the linear phase of aluminum uptake by excised roots of aluminum-tolerant and aluminum-sensitive cultivars. *Plant Physiol* **94**: 577–584
- Zhang G, Taylor GJ** (1991) Effects of biological inhibitors on kinetics of aluminum uptake by excised roots and purified cell wall material of aluminum-tolerant and aluminum-sensitive cultivars of *Triticum aestivum* L. *J Plant Physiol* **138**: 533–539